



HAL
open science

Easy methods to make the neuronavigated targeting of DLPFC accurate and routinely accessible for rTMS

Benjamin Pommier, François Vassal, Claire Boutet, Sophie Jeannin, Roland Peyron, Isabelle Faillenot

► To cite this version:

Benjamin Pommier, François Vassal, Claire Boutet, Sophie Jeannin, Roland Peyron, et al.. Easy methods to make the neuronavigated targeting of DLPFC accurate and routinely accessible for rTMS. *Neurophysiologie Clinique = Clinical Neurophysiology*, 2017, 47 (1), pp.35-46. 10.1016/j.neucli.2017.01.007 . hal-02138815

HAL Id: hal-02138815

<https://hal.science/hal-02138815>

Submitted on 4 Oct 2022

HAL is a multi-disciplinary open access archive for the deposit and dissemination of scientific research documents, whether they are published or not. The documents may come from teaching and research institutions in France or abroad, or from public or private research centers.

L'archive ouverte pluridisciplinaire **HAL**, est destinée au dépôt et à la diffusion de documents scientifiques de niveau recherche, publiés ou non, émanant des établissements d'enseignement et de recherche français ou étrangers, des laboratoires publics ou privés.

ORIGINAL ARTICLE

Easy methods to make the neuronavigated targeting of DLPFC accurate and routinely accessible for rTMS

Benjamin Pommier^{a,b,c,*}, François Vassal^{a,b,c}, Claire Boutet^d, Sophie Jeannin^e, Roland Peyron^{b,c,e}, Isabelle Faillenot^{b,c,e}

^aService de Neurochirurgie, Hôpital nord; F-42055 Saint-Etienne;

^bCentral Integration of Pain Unit – Inserm U1028 - Lyon Neuroscience Research Center - F-69000 Lyon ;

^cIntégration Centrale de la Douleur - Université Jean Monnet - F-42023 Saint-Etienne ;

^dService de NeuroRadiologie, Hôpital nord - F-42055 Saint-Etienne ;

^eService de Neurologie, Hôpital nord - F-42055 Saint-Etienne ;

Corresponding author:

Benjamin Pommier, Service de Neurochirurgie ; Hôpital Nord - F-42055 Saint-Etienne cedex 2

Phone : +33 477 127 805; Fax: +33 477 120 543; E-mail : benjamin.pommier@neurochirurgie.fr

Easy methods to make the neuronavigated targeting of DLPFC accurate and routinely accessible for rTMS

Abstract

Objectives: Dorsolateral prefrontal cortex (DLPFC) is the main stimulation target for rTMS treatment of depression. DLPFC is located in the middle frontal gyrus and corresponds to the lateral part of Brodmann Areas 9 and 46. Current methods to locate the DLPFC are either based on head landmarks that are inaccurate, or based on MRI-neuronavigation. Neuronavigated-methods are based either on standardized stereotactic coordinates translated to the individual patient or on brain landmarks requiring neuroanatomical skills for their identification. We developed a script automating the inclusion of already validated targets into patients' MRI, and also a new method to target DLPFC based on neuroanatomical landmarks. The present study aims to assess this new approach.

Methods: 4 targets were compared on 40 hemispheres: three previously validated methods (2 using superimposition of standardized targets on patient MRI and 1 using neuro-anatomical landmarks) and the new one presented here. Resulting targets were presented in the individual space and in stereotactic spaces (MNI and Talairach) with the main objective being to reach the middle frontal gyrus and BA9/46. Target dispersion and distances between targets were assessed.

Results: All targets were located in the middle frontal gyrus. Our proposed neuro-anatomical target was equivalent to or even better than the previously existing one if we consider the criteria of BA46 achievement and dispersion.

Conclusion: The proposed neuroanatomical method and automation of the stereotactic method allow simple and reliable targeting of DLPFC for rTMS treatment.

Keywords: Depression; DLPFC; Neuronavigation; Prefrontal Cortex; rTMS.

Running title: Neuronavigated targeting of DLPFC

Méthodes faciles pour rendre le ciblage neuronavigué du cortex préfrontal dorsolatéral précis et couramment accessible pour la pratique de la rTMS

Résumé

Objectifs: Le cortex préfrontal dorsolatéral (CPF DL) est la cible principale dans le traitement de la dépression par rTMS. Il est situé au sein du gyrus frontal moyen et correspond à la partie latérale des Aires de Brodmann 9 et 46. Les méthodes pour le localiser sont basées sur des repères externes (méthodes peu précises) ou des systèmes (complexes) de neuronavigation. Les méthodes de neuronavigation sont basées soit sur une translation de coordonnées stéréotaxiques standardisées vers l'IRM de l'individu, soit sur des repères anatomiques nécessitant des connaissances de neuroanatomie. Nous proposons d'une part un script permettant l'insertion automatique de cibles existantes dans l'IRM du patient, d'autre part une nouvelle méthode de ciblage par des repères anatomiques produisant une nouvelle cible que nous nous proposons d'évaluer.

Méthodes: 4 cibles ont été comparées sur 40 hémisphères en utilisant trois méthodes préalablement validées (2 utilisant des translations de cibles standardisées et une utilisant des repères anatomiques) et notre nouvelle méthode. Les cibles étaient déterminées dans l'espace de chaque patient et dans les espaces normalisés (MNI et Talairach). L'objectif était d'atteindre le gyrus frontal moyen et les aires de Brodmann 9 et 46. La dispersion des cibles et la distance les séparant étaient évaluées.

Résultats: Toutes les cibles se trouvaient dans le gyrus frontal moyen. Notre nouvelle cible anatomique était équivalente, voire supérieure, dans l'atteinte de l'aire 46. **Conclusion:** Nous présentons ici une nouvelle méthode anatomique et une automatisation d'une méthode stéréotaxique de ciblage du CPF DL pour la rTMS.

Mots-clés: Cortex préfrontal; CPF DL; Dépression; Neuronavigation; rTMS.

Introduction

The dorsolateral prefrontal cortex (DLPFC) is considered as an area of dysfunction in both depression and schizophrenia [8,11]. As such it is an important target for repetitive Transcranial Magnetic Stimulation (rTMS) both in a research context and in clinical treatment. Stimulating this target has been proven to be effective in major refractory depression [21,26][20,25] and it can also be used to modulate pain [5,32].

DLPFC is a very large cortical area, involved in various functions such as working memory and executive functions. However, defining an anatomical location from a functional definition is neither easy nor accurate. During the past decade rTMS targeting has been defined on the basis of the approximated “5-7 cm-method”: DLPFC was targeted 5 to 7 cm anterior to the primary motor cortex [16,20,21,26,27]. Although this is a quick and inexpensive method, it has been criticized since less than half of targets may actually be in the DLPFC [1,13,28]. It has since been proven that therapeutic results depend on targeting [6,9,24], leading to other methods aimed at improving targeting being proposed, such as the “10-20 method,” based on the international EEG system. The optimal DLPFC position thus defined according to the electroencephalogram 10-20 system seems to correspond to a point between F3 and F5 [31] or between F3 and AF3 if considering the Modified Combinatorial Nomenclature [7]. It has also given rise to different methods to simplify this approach [3]. However, these approaches seem to be insufficient, especially when compared to neuronavigation methods.[7]

Theoretically, DLPFC corresponds to the lateral part of Brodmann Areas (BA) 9 and 46 [3,7,29,31]. It is located within the superior (SFG) and middle (MFG) frontal gyri [8,14,33]. Generally, DLPFC is considered as being located in the middle part of the MFG [1,14,23,24] with occasional extensions to the SFG and rare extensions to the inferior frontal gyrus (IFG) [17]. Moreover, recent data using functional connectivity in resting-state

fMRI have suggested that BA46 appears to be the most functionally relevant area of the DLPFC to be targeted [9].

Neuronavigation is an essential tool allowing adequate placement of the rTMS coil and accurate targeting [2,6,12,18,19,30]. There are 3 main validated targets that can be integrated within the patient's MRI in different ways (Table 1, Figure 1): I/ targets defined in a standardized Talairach's space based on cytoarchitectonic findings [6,29]; II/ targets defined in a standardized Montreal Neurological Institute (MNI) space based on functional imaging [9] and III/ targets defined directly based on the individual patient's anatomy [23]. To include standardized targets into the patient's anatomical space, their coordinates need to be translated using spatial normalization (i.e. calculating parameters to match the patient's anatomy to a template). Commercially available tools can rapidly perform such transformations from standardized spaces. However, they carry out simple normalization with only linear transformations that remain encapsulated with precision that remains to be validated. Furthermore, they may be expensive. Conversely, research tools allow efficient normalizations, but their application may be complicated for untrained users. Neuroanatomical methods take individual anatomy into account, but for DLPFC, the only published method[23] might be difficult for people unskilled in neuroanatomy. Indeed, it requires a first step of identification of the olfactory sulcus and the middle frontal gyrus, which are known to be variable and can be responsible for up to 25% of mistakes [25]. Moreover, this method requires a peeling view of 3D-reconstruction of the individual brain, which is not available in all rTMS neuronavigation devices. For devices without surface rendering, a variant of this method has been previously published, but description of the method and definition of landmarks are not accurate [24].

With the hope of further improving the results of neuronavigated rTMS, we propose a freely available script automating the normalization process to add existing stereotactic

targets into patients' MRI. Moreover, we developed a new neuroanatomical method defining the DLPFC target using single-plan MRI slices. This provides a new DLPFC target that requires to be validated. To this aim we propose to assess this new target compared to the three previously published.

Methods

In individual patients, DLPFC can be defined with the following methods (Fig 1):

- **“stereotactic methods”**: stereotactically-defined targets are translated to the patient's individual anatomy through inverted-normalization [6,31]. The targets are defined either on a cytoarchitectonic basis as described by Rajkowska & Goldman-Rakic (called here **“Ref-R-GR”**) [29] or on a functional imaging basis [9] (called here **“Ref-Fox”**). In this paper, we will refer only to research normalization tools but not to commercially available systems. We propose to share the written script, which allows performing automated accurate non-linear normalization using the standalone version of SPM8 in order to insert these targets into the MRI of the patient. We stress that the released script simplifies the use of the existing stereotactic method but does not modify the targeting results, for which reason it will not be assessed.

- **the “neuroanatomic methods”**: for devices in which surface rendering is available, DLPFC targeting can be carried out using Mylius et al.'s description [23]. This defines a target that we have called here **“Ref-Mylius”**. We propose another neuroanatomical method that can be applied to any rTMS device without a peeling view of MRI. The resulting target is called here **“Prop-target”**.

To validate the new DLPFC target, its location should be in the middle frontal gyrus and preferentially in BA46. This target was compared to previously published targets by assessing distances from each another in individual spaces and coordinates in standardized spaces.

Please insert Table 1 and Figure 1 around here

Targets	Base	Space	References
Ref-R-GR	Cytoarchitectonic	Standardized	Rajkowska, 1995 Fitzgerald, 2009
Ref-Fox Ref-Mylius	Functional MRI Anatomical landmarks	Standardized Individual	Fox, 2012 Mylius, 2013
Methods	Advantages	Disadvantages	
Stereotactic (research tools)	Accuracy (non-linear transformations) Friendly interface	Unfriendly interface Encapsulated computation	
Stereotactic (trademark tools) Anatomical	No transformation of images	Linear transformations, Cost Learning neuroanatomy operator-dependent	

Subjects and MRI

This study enrolled 20 patients (11 women, 9 men) (40 hemispheres). The mean age was 51.8 years (min: 36; max: 78). After visual inspection of MRI, no subject presented significant morphological brain lesions.

All patients underwent a 3D T1-weighted MRI acquired either with a 1.5T or 3T magnet using a coil with 8, 12 or 32-channels. The sequence was the one proposed by the manufacturer (Siemens or Philips) with only 2 requirements: the resolution was 1x1x1 mm³ and axial slices were required to follow the bicallosal plane. All images were checked to be free of artifacts.

Target definition

Ref-R-GR, Ref-Fox and Ref-Mylius targets were considered here as “gold standards” because of their previous publications. Ref-R-GR target was originally defined in the Talairach space whereas Ref-Fox was described in MNI-Space. Therefore, we chose to describe all targets in both spaces.

The **Ref-R-GR target** was based on cytoarchitectonic work and is located between BA 46 and 9 as described by Rajkowska and Goldman-Rakic [29]. It lies at the Talairach coordinates (+/-45,45,35), corresponding to MNI coordinates (+/-46,45,38) [7].

The **Ref-Fox target** was based on functional connectivity and corresponds to the MNI coordinates (+/-44,38,34) [9] and to Talairach coordinates (+/-44,38,29).

Both of these stereotactically-defined targets were included in the individual MRIs using the automated script. First, two images were created with WFU-Pickatlas software [22], including 2 spheres of 2mm radius representing left and right Ref-Fox or Ref-R-GR in MNI space [4]. They were translated into the MRI of each patient using the “stereotactic method” as follows: the script was written in SPM8 software (fil.ion.ucl.ac.uk/spm) to apply an inverse normalization with the aim of automatically inserting the standardized targets into each patient’s MRI. The script consists of: I/ the segmentation of the patient’s brain to calculate its spatial normalization parameters (patient to MNI); II/ the spatial transformation of the target image using inverted parameters (MNI to patient); III/ the addition of both images. The output image is obtained automatically. It represents the chosen target by a white voxel on the brain of the patient. This procedure can be implemented in any neuronavigation system.

The **Ref-Mylius** targeting was described by Mylius et al. [23] using a neuroanatomic method. We first identified the MFG on the 3D surface rendering of the brain with the following landmarks: the anterior border was on the same coronal plane as the anterior margin of the olfactory sulcus; the posterior border was the pre-central sulcus; the inferior and superior borders were the inferior and superior frontal sulci. The Ref-Mylius target was then drawn on the brain surface (in the grey matter) at the middle of the line separating the anterior and middle third of the MFG. This method was applied to the 40 hemispheres of

the study. We used MRIcron software (www.mricro.com), which provides a 3D surface rendering of the brain.

The **Prop-target** results from a neuroanatomic method illustrated in Figure 2, which requires a 3-plan display provided by all neuronavigation systems. To develop this procedure, we carefully searched for invariable radiological landmarks that constantly localized to the middle prefrontal gyrus on numerous MRI other than those used in this study. These landmarks had to be invariable and easy to locate for people unskilled in neuroanatomy i.e. presenting important signal contrast and good visual reproducibility among patients. On the sagittal plane, the cursor is located immediately on the genu of the corpus callosum, defining the y-coordinate of the target. Then the axial plane is raised until the corpus callosum disappears and the cingulate cortex appears as a continuous cortical ribbon, defining the z-coordinate of the target. The intersection of the horizontal arms of the cross with the convexity of the cortical surface defines the x-coordinates (left and right). This procedure for DLPFC localization (Figure 2, Figure 3, and video) was repeatedly applied to the 40 hemispheres. This anatomical targeting was performed using MRIcron but can be achieved with any imaging software, particularly any rTMS neuronavigation software.

The Ref-Mylius and the Prop-target were saved as spheres of 2 mm radius inside the individual MRI space of the patient. With the aim of a comparative validation, this image was also normalized to the MNI space using the parameters provided by the SPM segmentation. The MNI coordinates of the targets were translated into the Talairach space using the algorithm proposed by WFU_Pickatlas software.

Considering all the procedures, we obtained 4 right and 4 left targets in 20 individual MRIs (each target in each individual patient MRI); 42 right and 42 left targets in MNI space; 42 right and 42 left targets in Talairach space (the stereotactically-defined Ref-R-

GR and Ref-Fox targets, and the results of the normalization of 20 left and right Ref-Mylius targets and 20 left and right Prop-targets in each one of the standardized spaces).

Please insert Figure 2 around here

Assessment of target validity

Visual/qualitative comparison of the targets

- **Gyral location:** Once the four targets were drawn in the individual space, their gyral locations were identified for each subject.
- **Cytoarchitecture estimation:** After MNI normalization, ref-Mylius and Prop-targets could be fused with images representing BA 46 and 9 (as provided by WFU_Pickatlas). This approach has been previously used by others [33]. After translation into Talairach space, targets could be reported on the original drawing proposed by Rajkowska et al. to determine their position regarding their definition of the cytoarchitecture of BA 9 and 46 [29].

Quantitative comparison of targeting

To check whether or not the locations of the Prop-target and the Ref-Mylius target were equivalent, three different analyses were conducted.

First, in individual space, Euclidian distances between each target were calculated. Mean distances between each anatomical target and each stereotactic target were compared using a paired t-test.

Secondly, to assess the between-subject variability in target localization, we compared the dispersion between coordinates in MNI-space (Fisher-Snedecor test,

variance comparison). To this aim, coordinates of both Prop-target and Ref-Mylius target were transformed (normalized) to fit the MNI space.

Thirdly, to define the relative positions of all these targets (i.e. superior/inferior and anterior/posterior), their y- and z- MNI-coordinates were compared. Since x-coordinates of the Prop-target were determined from the intersection between y and z planes, comparisons were performed only on y and z coordinates. Moreover, Ref-R-GR and Ref-Fox cannot be compared with one another as each one of them corresponds to a unique point in standardized spaces. The neuroanatomic targets (Ref-Mylius and Prop-target) were compared to each other using a paired t-test and they were compared to Ref-R-GR target and Ref-Fox target coordinates using a one-sample conformity t-test. All these tests were corrected with the Bonferroni method.

For all statistical analyses, data from the 40 hemispheres were considered as 40 independent measures. Quantitative values were presented as an average +/- standard deviation (SD) and qualitative values were presented with percentage of the sample. The statistical significance threshold was set to $p < 0.05$.

Results

Qualitative comparison

Individual space: Gyral location

Prop-targets were located in the middle frontal gyrus in the 40 hemispheres, as were the Ref-Mylius, the Ref-R-GR and the Ref-Fox target.

Normalized space: Cytoarchitectonic location

Figure 4 shows the projections of all targets on the surface of a MNI or a Talairach template, respectively. Stereotaxic coordinates and locations according to Brodmann

Areas are summarized in Table 2. The Prop-targets were mainly estimated in the BA46 whereas Ref-Mylius targets were closer to the border between BA46 and BA9.

Please Insert Table 2 around here.

Table 2 Mean MNI-coordinates of the Ref-Mylius and Prop-target and their cytoarchitectonical allocations.

	x	y	z	BA (WFU)	BA (R-GR)
<i>Prop-target</i>					
Mean	47.9	36.7	25	BA46: 40 (100%) BA9: 0 (0%) ND: 0 (0%)	BA46: 32 (80%) BA9: 0 (0%) ND: 8 (20%)
SD	4.4	3.6	4.2		
<i>Ref-Mylius</i>					
Mean	40.6	43.3	28.6	BA46: 17 (42.5%) BA9: 21 (52.5%) ND: 2 (5.0%)	BA46: 28 (70%) BA9: 3 (7.5%) ND: 9 (22.5%)
SD	3.1	4.8	5.3		

The Prop-target was mainly located in BA46 while Ref-Mylius targets was inconsistently located in this Brodmann area. This is true whatever the atlas used to localize cytoarchitectonic areas: WFU-Pickatlas (WFU) or the "Rajkowska and Goldman-Rakic's drawing" (R-GR, see Fig. 3). ND: not defined in these representations.

Please insert Figure 4 around here.

Quantitative Comparison

Individual space

Figure 5 shows the mean distances between the 4 targets in individual spaces. Prop-targets and Ref-Mylius were separated by about 12 mm on average. For the 40 hemispheres, Prop-targets were more distant from the Ref-R-GR than were the Ref-Mylius ($p=0.01$). Prop-target and Ref-Mylius were equally distant ($p=0.35$) from Fox-target on average (about 10mm). Detailed data are presented in Table 3.

Table 3 Mean euclidian distances (mm) between targets on the 40 hemispheres, in individual spaces.

	Prop-target	Ref-Mylius	Ref-R-GR
<i>Ref-Fox</i>			
Mean	9.9	10.1	9
SD	4.1	4	2.1
Min.	1	1.41	5.9
Max.	20.5	20	18.1
<i>Ref-R-GR</i>			
Mean	14.5	12	
SD	4.5	3.6	
Min.	5.8	6.2	
Max.	22.5	21.3	
<i>Ref-Mylius</i>			
Mean	11.6		
SD	4.4		
Min.	2.8		
Max.	22.3		

Please Insert Figure 5 around here.

Standardized spaces (MNI and Talairach)

Mean coordinates in MNI space are indicated in Table 2. All the coordinates obtained for each hemisphere in MNI space are shown in Table 4.

Table 4 MNI coordinates of the targets defined from anatomical landmarks (ref-Mylius and prop-targets) in the 20 subjects and their respective cytoarchitectonical location according to WFU-pickatlas.

Subject	ref-Mylius target								Prop-target							
	Left MNI coordinates			Location	Right MNI coordinates			Location	Left MNI coordinates			Location	Right MNI coordinates			Location
	X	Y	Z		X	Y	Z		X	Y	Z		X	Y	Z	
1	-42	46	24	46	40	46	28	46	-49	36	19	46	51	38	20	46
2	-44	42	28	46	42	42	34	46	-47	34	32	46	45	36	32	46
3	-45	44	19	46	41	44	28	9	-52	30	24	46	54	38	18	46
4	-46	48	20	46	42	46	26	46	-46	37	23	46	48	39	22	46
5	-35	47	37	9	36	47	31	9	-46	37	26	46	47	42	27	46
6	-41	33	30	46	40	42	32	46	-40	34	30	46	44	38	30	46
7	-39	38	37	9	39	46	30	9	-50	34	26	46	51	37	23	46
8	-35	42	38	9	41	44	37	9	-35	42	28	46	46	43	28	46
9	-38	36	35	9	44	47	24	46	-49	33	31	46	53	30	31	46
10	-44	41	29	46	42	42	24	46	-47	33	25	46	48	37	25	46
11	-42	47	30	9	42	51	27	9	-50	33	27	46	48	37	27	46
12	-35	37	33	9	37	42	28	9	-48	34	25	46	52	34	25	46
13	-42	31	30	9	46	38	34	9	-36	46	29	46	46	38	28	46
14	-35	38	37	9	41	38	20	9	-45	32	26	46	56	34	20	46
15	-39	48	27	9	42	48	27	9	-48	38	19	46	52	38	18	46
16	-44	45	26	46	44	50	21	46	-42	40	24	46	54	30	24	46
17	-39	42	29	9	41	42	33	9	-48	38	24	46	48	34	24	46
18	-41	51	18	46	42	50	29	9	-49	38	17	46	52	41	17	46
19	-41	42	21	46	44	38	27	46	-46	38	27	46	51	38	30	46
20	-36	48	26	Other	36	42	28	Other	-45	40	24	46	51	38	24	46
Average	-40.2	42.3	28.7		41.1	44.3	28.4		-45.9	36.4	25.3		49.9	37	24.7	
SD	3.6	5.4	6.2		2.6	4	4.3		4.5	3.8	3.9		3.3	3.4	4.5	

Although Ref-Mylius targets seem to lead to more dispersion, variances of the MNI-coordinates of the Mylius- and Prop-targets were not significantly different (Table 5).

Table 5 Dispersion analysis of both of the anatomical targets.

MNI-coordinates	Variance ref-Mylius	Variance Proposed target	P
y	12.7	23.0	0.07
z	17.4	28.2	0.14

Variance comparison, Fisher-Snedecor test.

Average positions of targets are significantly different across techniques since mean coordinates of the 4 targets were all significantly different from one another. Prop target is inferior and posterior to Ref-Mylius (Table 6). Prop-target was posterior and inferior to Ref-

R-GR, while the Ref-Mylius was only inferior. Prop-target was only inferior to Ref-Fox, while Ref-Mylius was significantly anterior and inferior to Ref-Fox. (Table 6).

Table 6 Relative positions of the different targets in MNI-space: mean coordinates difference (mm) between each target, and *P*-value of the coordinates comparisons.

	Ref-R-GR (mean \pm SD; <i>P</i>)	Ref-Fox (mean \pm SD; <i>P</i>)	Ref-Mylius (mean \pm SD; <i>P</i>)
<i>Ref-Mylius</i>			
Δy	-1.7 ± 4.8 ; 0.2	5.3 ± 4.8 ; 2×10^{-7}	
Δz	-9.4 ± 5.3 ; 6.3×10^{-13}	-5.4 ± 5.3 ; 8×10^{-7}	
<i>Proposed target</i>			
Δy	-8.3 ± 3.6 ; 1.2×10^{-16}	-1.3 ± 3.6 ; 0.2	-6.6 ± 5.9 ; 1.5×10^{-8}
Δz	-13 ± 4.2 ; 6.6×10^{-22}	9.0 ± 4.2 ; 1.8×10^{-16}	-3.6 ± 5.15 ; 8.5×10^{-5}

The difference corresponds to left column minus right column.

Discussion

Various methods exist for accurately locating a target in the DLPFC before starting an rTMS session with a neuro-navigation system displaying the individual MRI of the patients. This step is warranted for all rTMS studies designed for stimulating DLPFC, mainly because this region is not a clearly delineated cortical zone. It is also important to accurately define the target for repetition of sessions and for the reliability of targeting across sessions, investigators, or centers (in case of multi-center studies).

The two methods presented here have been developed in parallel but they are profoundly different in nature. We deliberately presented them together because they may concern different users of rTMS systems and because of their complementarity. The main advantages of these methods are their ease of use, their complementarity and their free access. We emphasize that the stereotactic method that we propose and make freely available is an automation of existing methods. It uses the two main existing and previously validated targets (Ref-R-GR and Ref-Fox) that we used as references throughout the article.

The stereotactic method provides an easily used script to target DLPFC, and potentially other targets in the brain. It has the following advantages over the proposed

neuroanatomical method: 1/ to exclude human manipulations in the definition of the target, 2/ to use an already validated target, 3/ to be independent from image orientation, 4/ to provide a controlled and validated normalization tool as compared to those provided by trademark solutions, and 5/ to be reproducible and easily translated from one site of investigation to the others in case of multicenter studies. As a disadvantage, the script and the SPM software (but not necessarily Matlab) must be installed and patients should not have any radiologically significant cerebral lesion.

If one considers that the stereotactic coordinates proposed previously for rTMS studies [6,7,31] are appropriate to stimulate DLPFC, the stereotactic method presented here can circumvent the limitations related to individual anatomy. The general principle of this method is based on a non-linear transformation of the individual brain to match a standard brain (MNI space). Performing this transformation in a clinical environment usually requires a neuroimaging background and is not generally appropriate for routine practice. For these reasons, the script is freely available at www.crn1.fr/data/DLPFCtarget_pommier and allows the automated inclusion of a dot representing the target in each patient MRI. This batch is written for the standalone version of SPM8 (which is freely available and does not require a Matlab license). Once SPM8 and the batch have been installed, the programme is fully automated.

It should be noted that the choice of Talairach coordinates for targeting cortical regions is not very reliable. The Talairach and Tournoux atlas was created based upon a single post-mortem dissection of a human brain. The MNI atlas, being based on 152 healthy subjects, includes inter-individual variability. Nevertheless, cytoarchitectonic data are rarely defined in stereotaxic spaces and even less in MNI space. Moreover, the Talairach to MNI transformation might bring some inaccuracy.

The use of individual functional data using a paradigm of working memory or connectivity [7,10] has been suggested and might be the best way to define the DLPFC. However, its clinical feasibility as a routine method remains hypothetical.

Apart from being an accurate tool for targeting this large cortical area, the methods described here provide reliable ways to define invariable targets across subjects, repetition of sessions, investigators, and centers.

The proposed neuroanatomical method provides a brand new target (the "Prop-target"). It is based on individual regional anatomy, defined by invariant and readily recognisable MRI landmarks. It requires only two manipulations of the MRI which can replace older processes based on external landmarks. As compared to previous anatomical targeting which can be considered as standard (providing Ref-Mylius target [23]), the method proposed here does not need any MRI transformation or computation. We tried to make it user-friendly for those without precise knowledge of local neuroanatomy and without need for trademark software for 3D-surface rendering. Moreover, it is based on reliable anatomical landmarks presenting important signal contrast from one another and good visual similarity among patients. On the other hand, the Ref-Mylius method localizes DLPFC as a part of the middle frontal gyrus, on the anatomical basis of superior and inferior frontal gyri. It should be noted that up to 32% of patients can present a long intermediate frontal sulcus, which can be mistaken for a superior or inferior sulcus [25]. In these conditions, it appears as an advantage that our proposed method provided targets consistently located in the MFG with an inter-subject variability that was similar for both neuroanatomical methods (similar variance comparison), without taking sulci into account.

Overall, both methods provided targets in MFG, with good clustering since their mean coordinates are all significantly different. Targets varied only around the junction

between BA9 and BA46. Prop-targets were more distant from the Ref-R-GR than was the Ref-Mylius, whose position was slightly more anterior and superior than the Prop-targets. If one considers depression and schizophrenia, functional imaging abnormalities have been described in a more posterior and lateral subdivision of the DLPFC than those defined by the ref-R-GR target [8,31]. Accordingly, Prop-target probably fits the pathophysiology of depression and schizophrenia as well as results of connectivity studies [9].

The main difference between our Prop-target and Ref-Mylius was that Prop-target was systematically located within BA46 while it was distributed in BA46 and BA9 for the Ref-Mylius target. Since fMRI data tend to suggest that the BA46 localization should be preferentially targeted [1,9,27], in addition to previously published anatomical localizations [22,29], this may be an advantage. Nevertheless, the clinical benefits of stimulating BA46 are not proven and should be investigated. If one wants to preferentially target the border between BA9 and BA46, the Ref-Mylius method is probably preferable.

DLPFC is a large functional region of the frontal lobe, which is not anatomically circumscribed and for which clear-cut borders are lacking. It corresponds to the intersection between the MFG and the lateral part of the SFG, and Brodmann Areas 9 and 46 [8]. These objective criteria were used to more precisely define DLPFC targets with respect to both frontal gyri (MFG) in the individual space, and projections of BA 9/46 on the cortical surface of the brain in standardized spaces (both MNI and Talairach spaces). Given the uncertainty by which the DLPFC target is generally defined, targeting with Prop-target could be relevant to ensure a Brodmann localization in a frontal area with unclear borders and functional delimitation. This method should contribute to more homogeneous targeting in future studies.

The main limit of this method is that axial slices need to be roughly oriented according to the bicommissural plane (AC-PC, also called the bicallosal plane) before

applying this neuroanatomical method. In cases of other orientation, reorientation of the MRI should be processed; otherwise priority should be given to the Stereotactic method.

Overall, the targets compared in this study reached the objective criterion of being part of the DLPFC with slight variation. They all present a moderate dispersion and are almost equally distant from one another (from 10 to 15 mm). This slight dispersion should be positively considered regarding rTMS spatial resolution estimated to a surface of around 2 cm² (18 mm diameter circle, [15]). Targeting procedures have proved to be reliable when locating the DLPFC with a limited inter-subject variability. In this stereotactic method, validated through normalization algorithms, the proposal of targets without human interference, and automatically superimposed on the patients' MRI, should be of interest to teams involved in multicenter or multi-investigator rTMS studies. More interesting is the reliability of targeting from one rTMS session to another and this result fit the necessary standardization of rTMS procedures. Finally, by using similar processes, it should be possible to define reliably any stereotactically defined targets in the brain.

Conclusion

The question is which of these two methods to choose? If the purpose is to achieve a standardized trial, including in multicenter studies, the stereotactic method will definitely have a better profile, on the basis of reliability between subjects, between sessions, and if relevant, between centers. Moreover, it provides different targets based on cytoarchitectonic or functional data. Conversely, if standardization is less important, the proposed neuroanatomical method could be applied without any difficulty to obtain a reliable and accurate BA46 targeting, because it takes into account individual anatomy. It will provide a target a little more anterior and inferior than the others, mainly located in

BA46. Subsequently it could be of interest to further assess its inter-rater reliability as well as its clinical significance.

Conflict of interest

To be completed by the authors.

References

- [1] Ahdab R, Ayache SS, Brugières P, Goujon C, Lefaucheur JP. Comparison of “standard” and “navigated” procedures of TMS coil positioning over motor, premotor and prefrontal targets in patients with chronic pain and depression. *Neurophysiol Clin* 2010;40:27–36.
- [2] Ayache SS, Ahdab R, Chalah MA, Farhat WH, Mylius V, Goujon C, et al. Analgesic effects of navigated motor cortex rTMS in patients with chronic neuropathic pain. *Eur J Pain* 2016;20:1413–22.
- [3] Beam W, Borckardt JJ, Reeves ST, George MS. An efficient and accurate new method for locating the F3 position for prefrontal TMS applications. *Brain Stimul* 2009;2:50–4.
- [4] Evans AC, Collins DL, Mills SR, Brown ED, Kelly RL, Peters TM. 3D statistical neuroanatomical models from 305 MRI volumes. In: Nuclear Science Symposium and Medical Imaging Conference, 1993. IEEE Conference Record. 1993. p. 1813–7. http://ieeexplore.ieee.org/xpls/abs_all.jsp?arnumber=373602
- [5] Fierro B, De Tommaso M, Giglia F, Giglia G, Palermo A, Brighina F. Repetitive transcranial magnetic stimulation (rTMS) of the dorsolateral prefrontal cortex (DLPFC) during capsaicin-induced pain: modulatory effects on motor cortex excitability. *Exp Brain Res* 2010;203:31–8.
- [6] Fitzgerald PB, Hoy K, McQueen S, Maller JJ, Herring S, Segrave R, et al. A randomized trial of rTMS targeted with MRI based neuro-navigation in treatment-resistant depression. *Neuropsychopharmacology* 2009;34:1255–62.
- [7] Fitzgerald PB, Maller JJ, Hoy KE, Thomson R, Daskalakis ZJ. Exploring the optimal site for the localization of dorsolateral prefrontal cortex in brain stimulation experiments. *Brain Stimul* 2009;2:234–7.
- [8] Fitzgerald PB, Oxley TJ, Laird AR, Kulkarni J, Egan GF, Daskalakis ZJ. An analysis of functional neuroimaging studies of dorsolateral prefrontal cortical activity in depression. *Psychiatry Res* 2006;148:33–45.
- [9] Fox MD, Buckner RL, White MP, Greicius MD, Pascual-Leone A. Efficacy of Transcranial Magnetic Stimulation Targets for Depression Is Related to Intrinsic

Functional Connectivity with the Subgenual Cingulate. *Biol Psychiatry* 2012;72:595–603.

- [10] Fox MD, Halko MA, Eldaief MC, Pascual-Leone A. Measuring and manipulating brain connectivity with resting state functional connectivity magnetic resonance imaging (fcMRI) and transcranial magnetic stimulation (TMS). *NeuroImage* 2012;62:2232–43.
- [11] Glahn DC, Ragland JD, Abramoff A, Barrett J, Laird AR, Bearden CE, et al. Beyond hypofrontality: A quantitative meta-analysis of functional neuroimaging studies of working memory in schizophrenia. *Hum Brain Mapp* 2005;25:60–9.
- [12] Herbsman T, Avery D, Ramsey D, Holtzheimer P, Wadjik C, Hardaway F, et al. More Lateral and Anterior Prefrontal Coil Location Is Associated with Better Repetitive Transcranial Magnetic Stimulation Antidepressant Response. *Biol Psychiatry* 2009;66:509–15.
- [13] Herwig U, Padberg F, Unger J, Spitzer M, Schönfeldt-Lecuona C. Transcranial magnetic stimulation in therapy studies: examination of the reliability of “standard” coil positioning by neuronavigation. *Biol Psychiatry* 2001;50:58–61.
- [14] Hoshi E. Functional specialization within the dorsolateral prefrontal cortex: A review of anatomical and physiological studies of non-human primates. *Neurosci Res* 2006;54:73–84.
- [15] Jalinous R. Technical and practical aspects of magnetic nerve stimulation. *J Clin Neurophysiol* 1991;8:10–25.
- [16] Janicak PG, Nahas Z, Lisanby SH, Solvason HB, Sampson SM, McDonald WM, et al. Durability of clinical benefit with transcranial magnetic stimulation (TMS) in the treatment of pharmacoresistant major depression: assessment of relapse during a 6-month, multisite, open-label study. *Brain Stimul* 2010;3:187–99.
- [17] John JP, Wang L, Moffitt AJ, Singh HK, Gado MH, Csernansky JG. Inter-rater reliability of manual segmentation of the superior, inferior and middle frontal gyri. *Psychiatry Res. Neuroimaging* 2006;148:151–63.
- [18] Lefaucheur JP. Why image-guided navigation becomes essential in the practice of transcranial magnetic stimulation. *Neurophysiol Clin* 2010;40:1–5.
- [19] Lefaucheur JP, Brugières P, Ménard-Lefaucheur I, Wendling S, Pommier M, Bellivier F. The value of navigation-guided rTMS for the treatment of depression: an illustrative case. *Neurophysiol Clin* 2007;37:265–71.
- [20] Leyman L, De Raedt R, Vanderhasselt MA, Baeken C. Effects of repetitive transcranial magnetic stimulation of the dorsolateral prefrontal cortex on the attentional processing of emotional information in major depression: A pilot study. *Psychiatry Res* 2011;185:102–7.
- [21] Loo CK, Mitchell PB. A review of the efficacy of transcranial magnetic stimulation (TMS) treatment for depression, and current and future strategies to optimize efficacy. *J Affect Disord* 2005;88:255–67.

- [22] Maldjian JA, Laurienti PJ, Kraft RA, Burdette JH. An automated method for neuroanatomic and cytoarchitectonic atlas-based interrogation of fMRI data sets. *NeuroImage* 2003;19:1233–9.
- [23] Mylius V, Ayache SS, Ahdab R, Farhat WH, Zouari HG, Belke M, et al. Definition of DLPFC and M1 according to anatomical landmarks for navigated brain stimulation: Inter-rater reliability, accuracy, and influence of gender and age. *NeuroImage* 2013;78:224–32.
- [24] Nauczyciel C, Hellier P, Morandi X, Blestel S, Drapier D, Ferre JC, et al. Assessment of standard coil positioning in transcranial magnetic stimulation in depression. *Psychiatry Res* 2011;186:232–8.
- [25] Ono M. *Atlas of the Cerebral Sulci*. Thieme Publishing Group; 1990.
- [26] O'Reardon JP, Solvason HB, Janicak PG, Sampson S, Isenberg KE, Nahas Z, et al. Efficacy and Safety of Transcranial Magnetic Stimulation in the Acute Treatment of Major Depression: A Multisite Randomized Controlled Trial. *Biol Psychiatry* 2007;62:1208–16.
- [27] Pascual-Leone A, Catalá MD, Pascual-Leone Pascual A. Lateralized effect of rapid-rate transcranial magnetic stimulation of the prefrontal cortex on mood. *Neurology* 1996;46:499–502.
- [28] Peleman K, Van Schuerbeek P, Luybaert R, Stadnik T, De Raedt R, De Mey J, et al. Using 3D-MRI to localize the dorsolateral prefrontal cortex in TMS research. *World J Biol Psychiatry* 2010;11:425-30.
- [29] Rajkowska G, Goldman-Rakic PS. Cytoarchitectonic definition of prefrontal areas in the normal human cortex: II. Variability in locations of areas 9 and 46 and relationship to the Talairach Coordinate System. *Cereb Cortex* 1995;5:323–37.
- [30] Ruohonen J, Karhu J. Navigated transcranial magnetic stimulation. *Neurophysiol Clin* 2010;40:7–17.
- [31] Rusjan PM, Barr MS, Farzan F, Arenovich T, Maller JJ, Fitzgerald PB, et al. Optimal transcranial magnetic stimulation coil placement for targeting the dorsolateral prefrontal cortex using novel magnetic resonance image-guided neuronavigation. *Hum Brain Mapp* 2010;31:1643-52.
- [32] Sampson SM, Kung S, McAlpine DE, Sandroni P. The use of slow-frequency prefrontal repetitive transcranial magnetic stimulation in refractory neuropathic pain. *J ECT* 2011;27:33–7.
- [33] Trojak B, Meille V, Jonval L, Schuffenecker N, Haffen E, Schwan R, et al. Interest of targeting either cortical area Brodmann 9 or 46 in rTMS treatment for depression: A preliminary randomized study. *Clin Neurophysiol* 2014;125:2384-9.

Figure Legends:

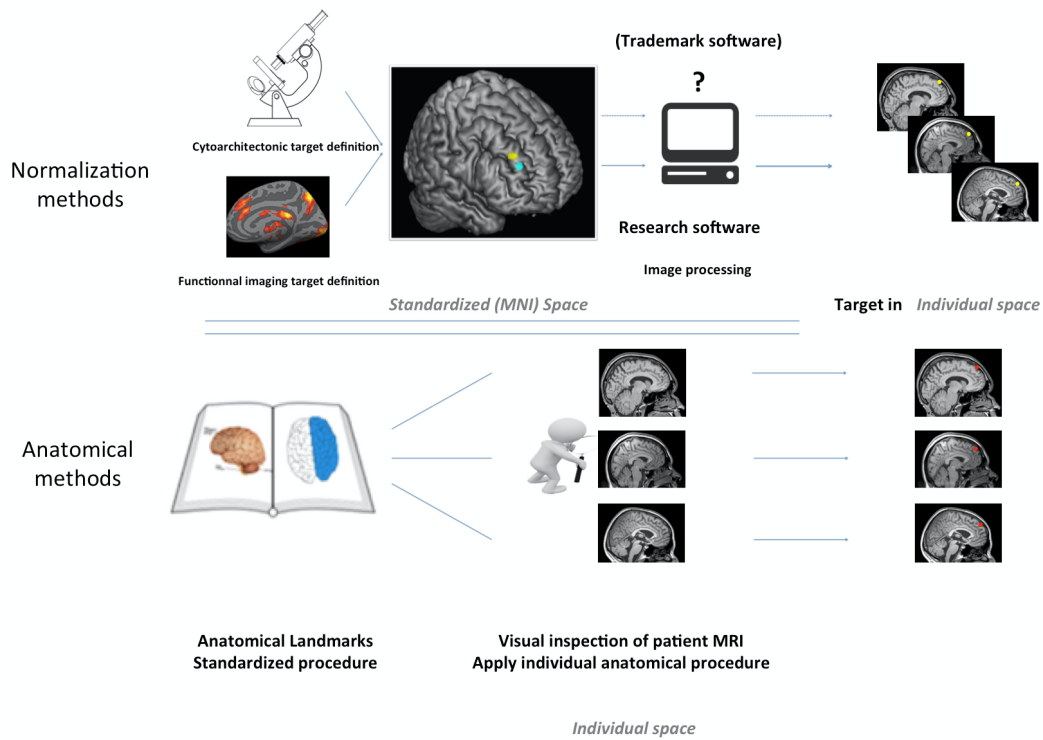


Figure 1: Different kinds of methods to determine the DLPFC target. Top row: Stereotactic method: After defining a target in the standardized space (x, y, z coordinates, blue and yellow dots) based on cytoarchitectonic or functional imaging data, translation of the coordinates in the individual space of the patients can be performed with either trademark devices or research software. Then these coordinates can be projected on individual MRIs to place the rTMS coil and deliver the stimulation on the target. Bottom row: Neuroanatomical way: Localization of the target is obtained by using external landmarks or sulci identification according to previous anatomical description. This method is directly performed on the individual MRI of the patient without any deformation but it requires anatomical skills and it is an operator-dependent step.

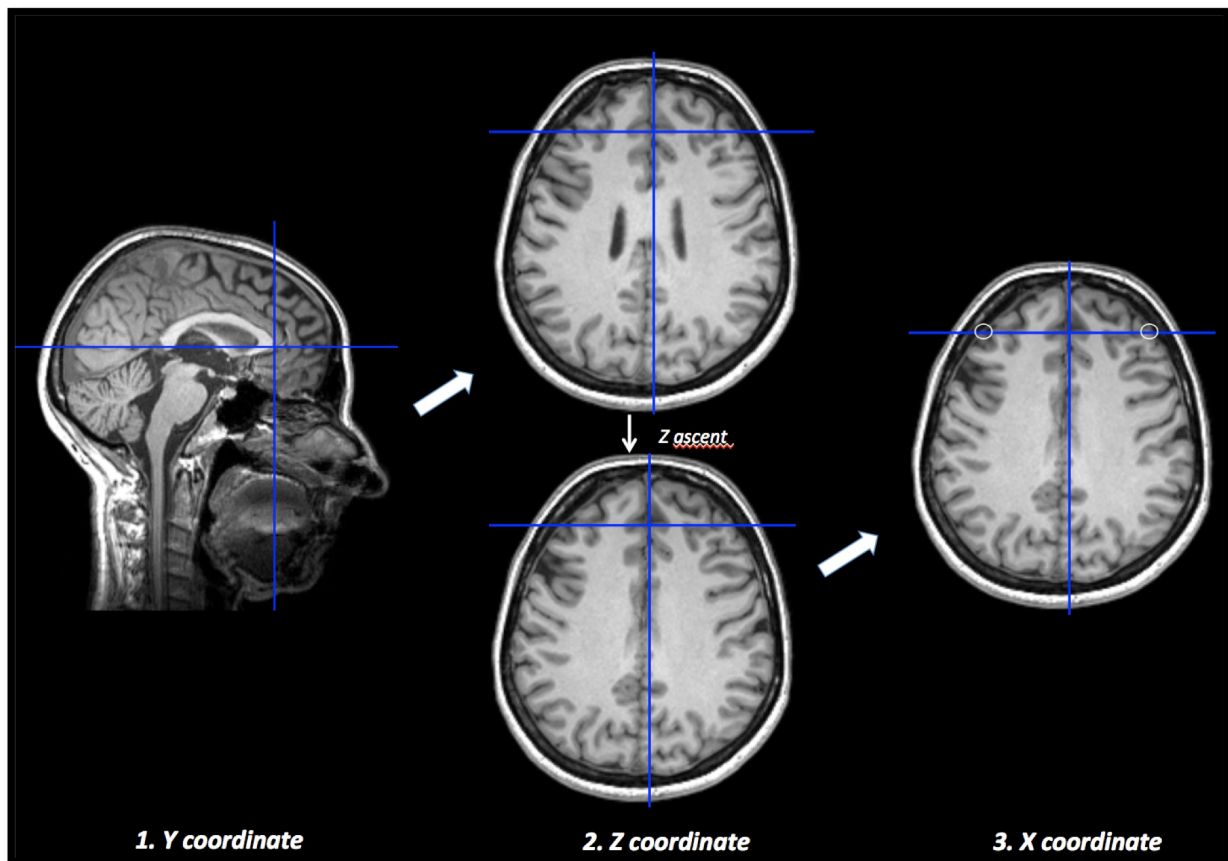


Figure 2: Our proposal for a neuroanatomical method to determinate DLPFC target (Prop-target) on individual MRI. The axial plane is almost parallel to the bicommissural (AC-PC) plane. 1/ Place the cursor on the genu of the corpus callosum; 2/ Drag up the axial plane until the corpus callosum disappears and the gray matter forms a continuous ribbon in the middle of the brain; 3/ Draw the R and L targets at the intersections of the coronal plane with the brain surface. Please note that only 2 manipulations are necessary to achieve the target.

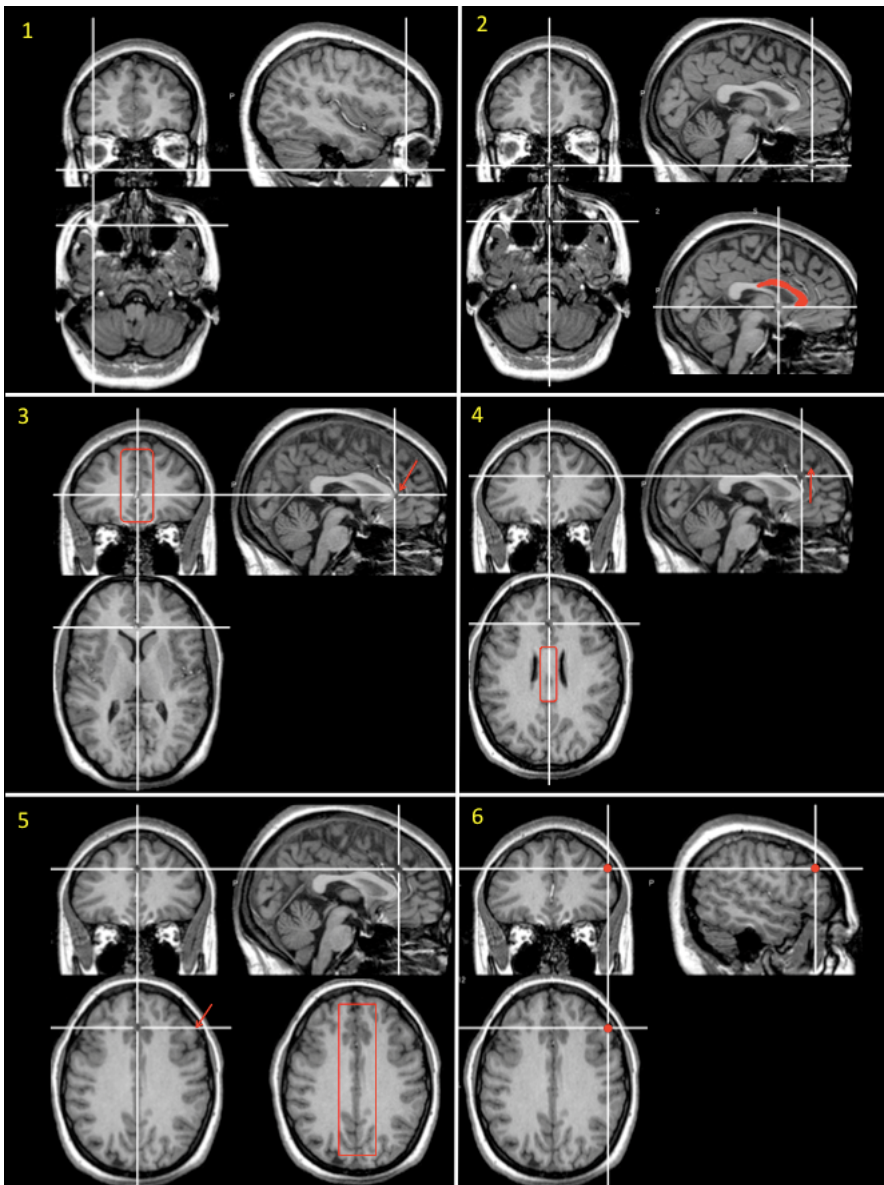


Figure 3: Our proposal for a neuroanatomical method to determine a DLPFC target (Prop-target) on individual MRI. Description of the “step by step” procedure as explained to people unskilled with neuroanatomy.

1/ First, open the MRI with the neuronavigation software.

2/ Check the images orientation:

- Place the cursor on a slide between the eyes.
- Find the front of the corpus callosum (filled in red on the figure) and place the horizontal cursor under it.

- Both extremities (arrows) of the corpus callosum should be closed from the horizontal line.

3/ Place the cursor just in front of the corpus callosum (arrow). Grey mater should be continuous in the coronal plane (as surrounded in red).

4/ Move the axial plane upward (arrow) until the corpus callosum disappears (When the white part surrounded in red disappears to become a continuous grey cortical ribbon).

5/ Don't move anymore when there is a continuous grey cortical ribbon on the axial plane as surrounded in red. Click at the cross of the brain surface and the horizontal line of the cursor (arrow).

6/ Place the target at that point (red point).

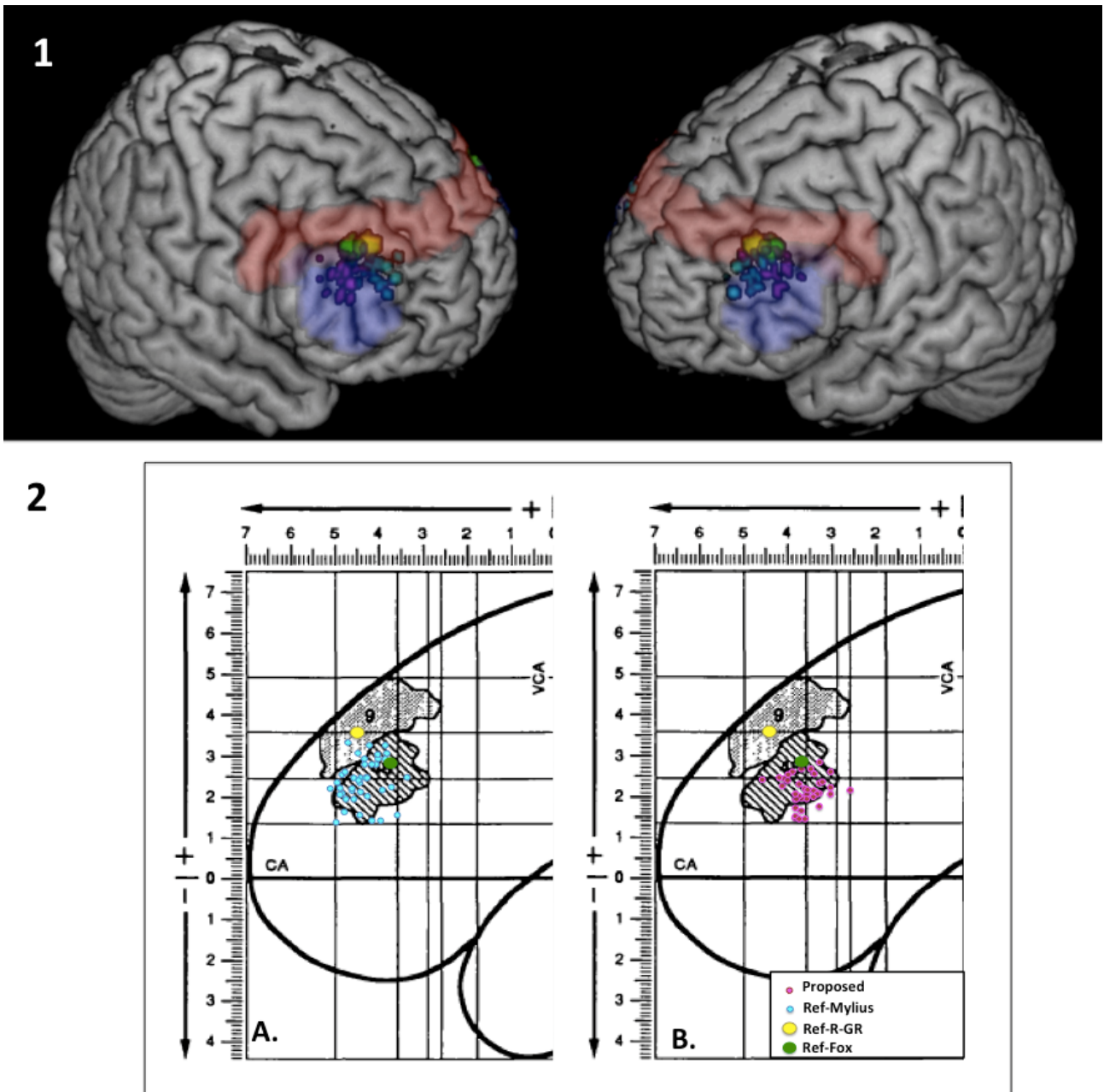


Figure 4: All DLPFC-targets superimposed on templates. Yellow dot: Theoretical Ref-R-GR target (Stereotactic method); Green dot: Theoretical Ref-Fox target (Stereotactic method); Cyan dots: Ref-Mylius targets (existing Neuroanatomical method); Purple dots: Prop-targets (proposed Neuroanatomical method).

1/ MNI-template 'ch2' from MRICron with BA9 (red) and BA46 (blue) provided by wfu_pickatlas; Here coordinates of the targets were in MNI space.

2/ Talairach grid space adapted from Rajkowska and Goldman-Rakic (1995) with graphic representation of BA9 and BA46 in gray. Here coordinates of the targets were transformed to fit the Talairach space.

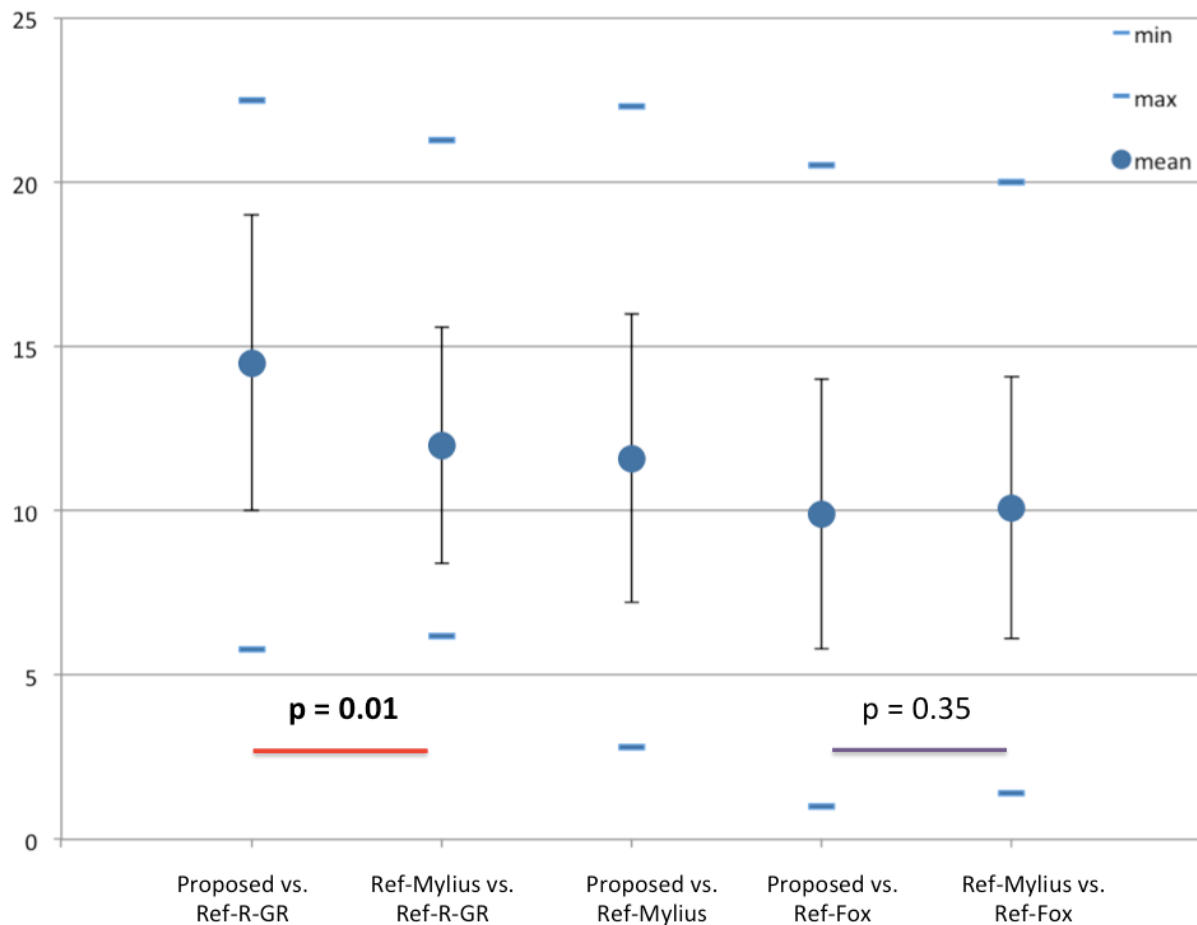


Figure 5: Mean euclidian distances (mm, +/-SD) between targets on the 40 hemispheres, in individual spaces. Distances between neuroanatomical targets and stereotactical targets are compared. Prop-target is significantly further from ref-R-GR (14.5mm (+/-4.5)) than ref-Mylius (12mm (+/- 3.6)). Prop-target is not significantly further from ref-Fox (9.9mm (+/-4.1)) than ref-Mylius (10.1mm (+/- 4)).